

Soil organic matter as affected by the conversion of natural tropical rainforest to monoculture rubber plantations under acric ferralsols

D. Balasubramanian^{a,b}, Yi-Ping Zhang^{a,b,*}, John Grace^c, Li-Qing Sha^{a,b}, Yanqiang Jin^d, Li-Guo Zhou^{a,b,e}, You-Xing Lin^{a,b,e}, Rui-Wu Zhou^{a,b,e}, Jin-Bo Gao^{a,b,e}, Qing-Hai Song^{a,b}, Yun-Tong Liu^{a,b}, Wen-Jun Zhou^{a,b,**}

^a CAS Key Laboratory of Tropical Forest Ecology, Xishuangbanna Tropical Botanical Garden, Chinese Academy of Sciences, Xishuangbanna 666303, China

^b Center of Plant Ecology, Core Botanical Gardens, Chinese Academy of Sciences, Xishuangbanna 666303, China

^c School of GeoSciences, The University of Edinburgh, Edinburgh EH9 3JN, UK

^d CAS Key Laboratory of Tropical Plant Resources and Sustainable Use, Xishuangbanna Tropical Botanical Garden, Chinese Academy of Sciences, Xishuangbanna 666303, China

^e Graduate University of the Chinese Academy of Sciences, Beijing 100039, China

ARTICLE INFO

Keywords:

Land-use change
Land degradation
Soil organic matter stability
Soil aggregate-size
density-size SOM fractions
Stable isotopes

ABSTRACT

Land-use change (LUC) in the tropics, such as the exponential rate of conversion of natural habitats into intense monocultures focusing on cash-crop cultivation, is a major causal factor of global environmental change. To understand the effects of LUC on soil organic matter (SOM) stability and the dynamics of C and N within SOM fractions, we measured the C and N content and $\delta^{13}\text{C}$ and $\delta^{15}\text{N}$ in fractions of different aggregate- and density-size of acric ferralsols in tropical rainforests and rubber plantations. The proportion of macroaggregates, heavy and light fractions significantly decreased after LUC. The results showed that, in general, conversion of tropical rainforest to rubber plantation significantly decreased the C and N content in bulk soil and the aggregate- and density-size to 20 cm soil depth. The decrease in C and N content in bulk soil was mainly driven by decreasing C and N associated with macroaggregates and light fractions, which accounted for > 50%. We found significant correlations among mean weight diameter, aggregate-, and density-size fractions C, N, and C/N ratios. The conversion of tropical rainforest to rubber plantation significantly enriched soil $\delta^{13}\text{C}$ while depleting $\delta^{15}\text{N}$. Enrichment of $\delta^{13}\text{C}$ in rubber plantations could be explained by the mixing of old and fresh C. We conclude that, C and N dynamics within SOM fractions were greatly affected by LUC and the $\delta^{13}\text{C}$ and $\delta^{15}\text{N}$ signature confirms the changes in SOM stability after forest conversion. We suggest that planting intercrops within rubber monocultures may improve SOM accumulation, soil aggregation, and C and N sequestration.

1. Introduction

The soil in rainforests stores much of the C of tropical regions in the form of soil organic matter (SOM). It is estimated that around 1550 Pg of organic C is stored in this form, twice as much as the C stored as CO_2 in the atmosphere (Zandi et al., 2017). SOM influences soil structure and functions in terms of physical properties, nutrient fluxes, and moisture retention. In general, SOM dynamics are predominantly controlled by climate, soil properties, and land-use management. Furthermore, land-use change (LUC) may lead to losses of C and N from SOM (Trumbore et al., 2015; Poeplau et al., 2011; Veldkamp et al., 2008).

Soil aggregates are basic ‘building-blocks’ of soil structure and vary in physicochemical properties; they are highly sensitive to LUC (Von Lütow et al., 2008). Physical disruption of soil aggregates during LUC exposes SOM surfaces to microbial decomposers, which results in the mineralization of stabilized SOM (Oades, 1995). Therefore, maintaining SOM levels is important for sustainable use and soil fertility.

Conversion of natural forest to plantations severely affects the quality and quantity of SOM and thereby its ecological functions. However, previous studies have reported contrasting effects of LUC on C, including increasing (Maggiotto et al., 2014), decreasing (Chiti et al., 2014), and having no effect on soil C (Frazão et al., 2013). LUC-driven

* Corresponding author at: CAS Key Laboratory of Tropical Forest Ecology, Xishuangbanna Tropical Botanical Garden, Chinese Academy of Sciences, Xishuangbanna 666303, China.

** Corresponding author at: Center of Conservation Biology, Core Botanical Gardens, Chinese Academy of Sciences, Xishuangbanna 666303, China.

E-mail addresses: yipingzh@xtbg.ac.cn (Y.-P. Zhang), zhouwj@xtbg.ac.cn (W.-J. Zhou).

<https://doi.org/10.1016/j.catena.2020.104753>

Received 31 July 2019; Received in revised form 19 May 2020; Accepted 5 June 2020

Available online 16 June 2020

0341-8162/ © 2020 Elsevier B.V. All rights reserved.

C and N loss can occur in different ways: (1) changing turnover rates with shifting decomposer communities, (2) low quantity and quality of above- and belowground plant litters, (3) increasing decomposition rates of labile C and N, or (4) erosive soil loss driven by aggregate-size disruptions and lack of physical binding agents such as plant litters. The inherent mechanisms of LUC effect on SOM stability depend upon vegetation type, including whether the plantation is monoculture (Rahman et al., 2019; Sierra and Desfontaines, 2018; Jandl et al., 2015).

SOM decomposition and stabilization can be assessed from the quality and quantity of different soil aggregate-sizes within the bulk soil by fractionation according to the size of aggregates (Cotrufo et al., 2013; Tisdall and Oades, 1982). The aggregate hierarchical model (Tisdall and Oades, 1982) shows that macroaggregates are highly unstable and prone to rapid decomposition, whereas microaggregates and organic-mineral particles of silt and clay size are relatively stable. Moni et al. (2012) suggested that a combination of particle size and density fractionation methods can significantly separate functional SOM pools. This would help in determining the aggregate-size fractions that are the main driving force behind overall bulk soil C and N dynamics after LUC. Although the aggregate- and density-size fractionations of SOM can give a crude estimation of the effect of LUC on SOM, there remains uncertainty concerning the underlying mechanisms of SOM dynamics following LUC. Natural abundance of $\delta^{13}\text{C}$ and $\delta^{15}\text{N}$ within individual SOM fractions reflect the degree of decomposition of SOM in relation to LUC (Christensen, 2001). Measuring C and N concentration within individual SOM fractions and $\delta^{13}\text{C}$ and $\delta^{15}\text{N}$ natural abundance can explain the underlying mechanisms of C and N dynamics after LUC (Blagodatskaya et al., 2011). Thus, parameters of SOM stability can be investigated by comparing C and N concentration with isotopic signatures.

Rubber (*Hevea brasiliensis*) is a major plantation crop and much natural tropical rainforest (TF) has been converted to monoculture rubber plantations (RP), in Southeast Asia, where 97% of the world's natural rubber is produced (Zhai et al., 2015). Large-scale conversion of TF into monoculture RP is common in the southern regions of China, as well as globally (Kurniawan et al., 2018; Guillaume et al., 2015; Chiti et al., 2014). The expansion of RP has increased by 20.9–22.1% in Xishuangbanna region between 1970 and 2010 (Zhai et al., 2017) while in last 4 decades, natural forest cover has decreased by > 30% (Zhai et al., 2017). Although the conversion of TF to RP changes soil C and N storage (Li et al., 2013), its underlying mechanisms are yet to be fully understood.

In the present study, to elucidate the effect on SOM dynamics of TF conversion to RP, we quantitatively determined the changes in SOM fractions of different aggregate- and density-size and measured soil C and N and their respective isotopic abundances of $\delta^{13}\text{C}$ and $\delta^{15}\text{N}$ in bulk soil. Our main aim was to test the following hypotheses: i) variation in C will result in decreased aggregate-size stability by decreasing the proportion of light fraction (LF) and macroaggregates (> 250 μm) fractions, and ii) LUC will induce soil $\delta^{13}\text{C}$ and $\delta^{15}\text{N}$ abundance shift, which will explain the C storage and stability in TF and RP.

2. Materials and methods

2.1. Study sites and experimental design

The experimental sites were in Xishuangbanna, in Yunnan province, southwestern China (21°55' 30" N, 101°15' 59" E). The study location is strongly influenced by the southwest tropical monsoon from the Indian Ocean, with mean annual temperature and annual precipitation of 22 °C and 1557 mm, respectively. The dry season is between November and April. From May to October is the wet season with > 85% of the total annual rainfall. The soil type is oxisol (United States Department of Agriculture (USDA)) or acric ferralsols (World Reference Base (WRB)) and formed from Cretaceous yellow sandstone and about 1 m

deep (Zhou et al., 2016a; 2016b). The dominant trees in TF include *Terminalia myriocarpa*, *Pometia tomentosa*, *Gironniera subaequalis*, *Barbingtonia macrostachya*, and *Garcinia cowa*. The rubber tree monocultures are cultivated on terraces (Cao et al., 1996). The RP sites were converted from TF in 1994. Mean canopy height is ~ 45 m in TF and it ranged from 20 to 30 m in RP (Zhou et al., 2016a; 2016b). The land cover ratio for RP and TF was 70 and 100%, respectively. While TF were relatively undisturbed, RP was subjected to land management, such as latex tapping, fertilizer application, and moderate removal of shrubs and the herbaceous layer. Rubber trees were planted 2 m apart in rows. The spacing between adjacent rows was either 3 m or 19 m. The trees were planted at a density of 495 rubber trees/ha. Rubber trees were tapped from March to November on alternate days. The latex was tapped ~ 110–125 times/year. Commercial fertilizer (Hubei Sanning Chemical, Yichang, China) was applied (0.5 kg N/tree/application) twice annually: once during the dry season at the end of March and once during the rainy season at the end of August (Zhou et al., 2016b).

2.2. Soil sampling and processing

The sampling plots were within 23 ha and 20 ha areas of TF and RP, respectively. Three plots (1 m × 2 m quadrants) from TF and RP were randomly selected. For SOM fractionation, five undisturbed soil cores (2.5 cm inner diameter) from 0 to 10 cm and 10–20 cm soil layers were collected randomly within three plots of both TF and RP in May 2017. The five soil samples were then mixed homogeneously according to plot and depth to provide one sample per replicated plot. At each sampling point, ~500 g of soil was collected. The mixed soils were divided into two parts and used for aggregate- and density-size fractionation of SOM. In addition, three intact soil cores from each plot under both sites were also collected for measuring pH and bulk soil C and N content, and $\delta^{13}\text{C}$ and $\delta^{15}\text{N}$. Samples were processed in the laboratory immediately after collection (Zhou et al., 2015). Visible larger rock and plant fragments were removed before sieving through a 2-mm mesh.

2.3. SOM fractionation

2.3.1. Aggregate-size fractionation

Water-stable aggregate (WSA) fractions (> 2000 μm , 2000–250 μm , 250–53 μm , and < 53 μm) were separated by wet-sieving (Figure S1a) using the method described by Cambardella and Elliott (1992). Briefly, three replicates of 100 g of fresh soil were transferred to a stack of sieves consisting of 2000 μm (top), 250 μm (middle), and 53 μm (base) meshes. This stack of sieves was then immersed in a bucket of Milli-Q water for 10 min at room temperature (25 °C). The sieve stack was raised and then the soil in the 2000 μm sieve was sieved under Milli-Q water by raising and lowering the stacks for 10 min with 30 cycles per min. Floating plant debris was removed, and the remaining water in the bucket was centrifuged (448 g for 15 min). The filtrate materials were considered as < 53 μm aggregate fractions. WSA fractions retained in each sieve were oven-dried at 40 °C for 48 h and weighed to measure percentage mass distribution of each WSA fraction in the bulk soil.

2.3.2. Density fractionation

Density gradient fractions (heavy fraction (HF) > 1.80 g cm⁻³, occluded LF (OLF) < 1.80–> 1.60 g cm⁻³ and light fraction (LF) < 1.60 g cm⁻³) were separated by sodium iodide (NaI) solution (Figure S1b). The density of NaI was gravimetrically adjusted to 1.80 g cm⁻³ and 1.60 g cm⁻³. These density ranges were selected based on previous studies (Griepentrog and Schmidt, 2013; Sohi et al., 2001). Multiple replicates (n = 15) of density fractionation were carried out for each soil sample in order to obtain sufficient SOM fractions for further chemical analyses. Fractions were pooled by density before subsampling for chemical analysis.

A subsample of each 15 g of 2-mm-mesh-sieved soil was transferred to a centrifuge tube and 50 mL of NaI (1.80 g cm⁻³) was added slowly.

The tube was gently swirled upside down by hand about 10 times to ensure the soil sample was completely suspended in NaI. Then the contents were centrifuged at 2800 g for 30 min at room temperature (25 °C). All material floating (LF) in the tube was decanted via a vacuum filter (Whatman GF/F-pore size: 0.45 µm). The decanted LF was rinsed multiple times with Milli-Q water to remove the excess NaI residues. The centrifugation process was repeated until all the floatable LF was completely separated from the HF. The material retained in the centrifuge tube was augmented with fresh NaI with a density of 1.60 g cm⁻³. The filtrate containing the HF was sonicated for 15 min with dispersing energy of 1500 J g⁻¹ soil at room temperature (25 °C) and centrifuged at 2800 g for 30 min. The floating OLF was recovered by decanting through a vacuum filter and washed as described above for LF. The centrifugation process was repeated until there was no further floating material. Finally, the filtrate remaining in the centrifuge tubes was rinsed with Milli-Q water repeatedly as described above. The density of the NaI after each extraction was determined by hydrometer and adjusted to 1.80 g cm⁻³ or 1.60 g cm⁻³ if there was any change in density. Density fractions were oven-dried at 40 °C for 48 h and weighed for the measurement of percentage mass distribution of each density fractions within the bulk soil.

2.4. Soil physicochemical analyses

Soil pH was measured potentiometrically (1:2.5 soil:H₂O) using a digital pH meter (FE28, Mettler Toledo, USA). Soil texture was measured by the pipette method that separated whole soil into sand (500–2000 µm), silt (200–500 µm), and clay (200 µm), and the textural class was determined according to the USDA classification system. Three additional intact soil cores from each plot in both sites were collected for measuring bulk density of fine earth (BD) gravimetrically based on the inner diameter of the soil core, sampling depth, and the oven-dried weight of the bulk soil by the following equation (Allen, 1989):

$$BD(gcm^{-3}) = \frac{D_w - G_w(g)}{S_v - G_v(cm^3)} \quad (1)$$

where D_w and S_v are oven dried soil core weight and soil core volume, respectively. Similarly, G_w and G_v are the dry weight of gravel content and gravel volume, respectively. Volume of the gravels were determined by filling 1/3 of a graduated measuring cylinder with water and recorded the volume (mL). Gravel fragments were added to the measuring cylinder and recorded the raise in the water level. Finally, the differences in the volume is the volume of gravels (1 mL = 1 cm³). Although gravel contents are negligible in our soil samples, we have included gravel contents in the formula in order to represent its originality. Soil water content (SWC) and soil temperature at 5 cm depth were recorded using a pre-calibrated time domain reflectometry (TDR) sensor (SM150, Delta-T Devices Ltd., Burwell, Cambridge, UK) and thermocouple probe (MHP; Omega Engineering Inc.), respectively. Based on the aggregate-size fractions recovered through wet sieving, the SOM stability index was measured as WSA, mean weight diameter (MWD), and geometric mean diameter (GMD). The MWD and GMD were calculated using the following equations (Six et al., 1998):

$$WSA = \frac{\text{Weight of wet} - \text{sieve resistant aggregates}(g)}{\text{Whole soil weight}(g)} \times 100 \quad (2)$$

$$MWD = \sum_{i=1}^n X_i \times W_i \quad (3)$$

$$GMD = \exp\left(\frac{\sum_{i=1}^n W_i \log X_i}{\sum_{i=1}^n W_i}\right) \quad (4)$$

where ' X_i ' is the mean of the diameter of the WSA retained on each sieve and ' W_i ' is the proportion of the retained WSA aggregates mass on each sieve to the total mass of bulk soil and ' n ' is the number of sieves used in

wet-sieving.

Subsamples were taken in triplicate from fractions of different aggregate- and density-size and bulk soils and were finely milled and analyzed for total C, N, $\delta^{13}C$ ($^{13}C/^{12}C$), and $\delta^{15}N$ ($^{15}N/^{14}N$). Total C and N content were determined using an element analyzer (Vario MAX CN, Elementar Analysensysteme GmbH, Germany). Natural abundances of $\delta^{13}C$ and $\delta^{15}N$ were measured using IsoPrime100 (UK) Isotope Ratio Mass Spectrometer (IRMS) coupled with Vario ISOTOPE cube (Elementar Analysensysteme GmbH, Germany). Ratios of C and N isotopes were expressed in parts per thousand (‰) relative to the differences from ratios of the standard Pee Dee Belemnite and atmospheric N ($^{15}N_{air}/^{14}N_{air} = 0.0036765$), respectively. The $\delta^{13}C$ and $\delta^{15}N$ were calculated as follows:

$$\delta^{13}C \text{ or } \delta^{15}N = \left(\frac{^{13}C \text{ or } ^{15}R_{\text{sample}}}{^{13}C \text{ or } ^{15}R_{\text{standard}}} - 1 \right) \times 1000 \quad (5)$$

where R is the molar ratio $^{13}C/^{12}C$ or $^{15}N/^{14}N$. Experimental error for isotopic standards was < 0.1‰ and 0.3‰ for $\delta^{13}C$ and $\delta^{15}N$, respectively. The total C and N associated with each fraction were calculated by multiplying the concentration of total C and N in particular fractions (g) by the total mass of bulk soil (g). Nutrient (C or N) loss from a particular fraction was calculated by deducting nutrient concentration within individual fractions from bulk soil nutrients. The concentration of C and N associated with bulk soil as well as different fractions were sand corrected by the following formula:

$$\text{Sand-free C or } N_{\text{fraction}} = C \text{ or } N_{\text{fraction}} / (1 - (\text{sand proportion}_{\text{fraction}})) \quad (6)$$

2.5. SEM analysis

Sub-structure of samples from different density fractioned soils were examined under the scanning electron microscope (SEM) to demonstrate the likely disruption in soil structure in response to the conversion of TF to RP. The samples were oven-dried and fixed on sticky C tape mounted on metallic stubs. The samples were then metalized with gold (Q150R-S Sputter coater, Quorum Technologies Ltd., Laughton, UK). SEM analyses of SOM fractions was performed using ZEISS EVO® LS 10 (Carl Zeiss, Oberkochen, Germany). The gun voltage was set to 10 kV with a vacuum pressure of $3 \times 16e^{-006}$ mbar.

2.6. Statistical analysis

Our data included two independent variables (land use and soil depth) and each composed of two categories (land use: TF and RP, soil depth: 0–10 and 10–20 cm layers). Normality of the variables was assessed using the Kolmogorov-Smirnov test prior to two-way analysis of variance (ANOVA) in STATISTICA 8.0 (StatSoft Inc., Tulsa, OK, USA). Statistical analyses were performed by two-way ANOVA with least-significant difference (LSD) statistics with a p -value threshold of 0.05 to examine significant variation among dependent variables, such as percentage mass proportion of fractions with different aggregate- and density-size, and associated C and N content, and $\delta^{13}C$ and $\delta^{15}N$ abundance between two independent variables, i.e., land-use (TF vs RP) and soil layers (0–10 vs 10–20 cm). All figures were drawn in OriginPro 8.0 (OriginLab Corporation, Northampton, MA, USA) and Excel 2018 (Microsoft Inc., Redmond, WA, USA). The Pearson's correlation coefficient (r) was determined to explain the relationships between the bulk soil, aggregate- and density-size fractions associated C and N, $\delta^{13}C$, and $\delta^{15}N$ abundance.

3. Results

3.1. Morphology of density fractionated SOM

Fig. 1 shows SEM images of density-separated SOM fractions (0–10

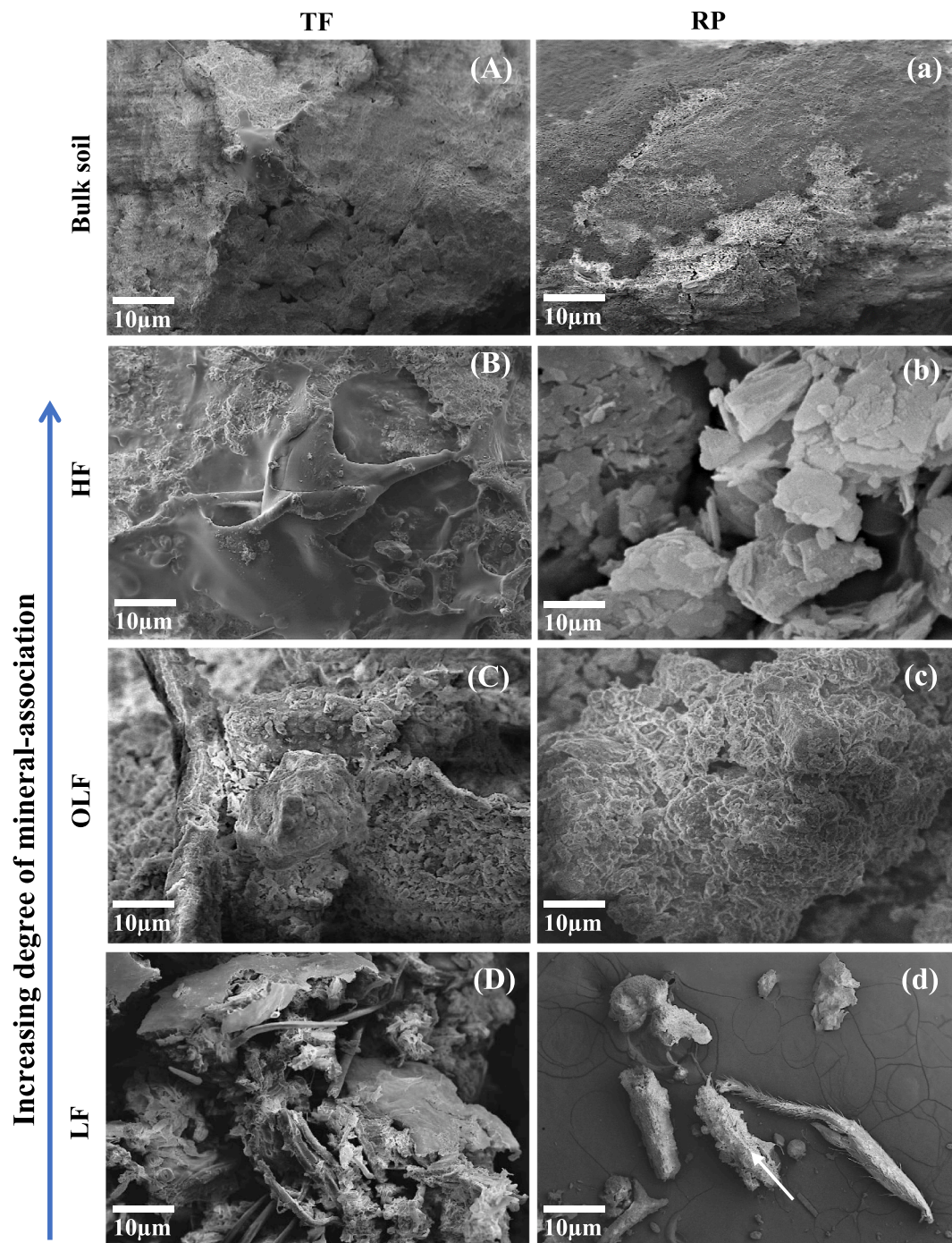


Fig. 1. Scanning electron microscope (SEM) observations of bulk soil and different density-size fractions (HF, OLF and LF) under tropical rainforest (TF) (A, B, C, D) and rubber plantations (RP) (a, b, c, d) at 0–10 cm soil depth. Bar = 10 µm. Image 2A (TF) and 2a (RP) is undisturbed bulk soil. Heavy fractions (HF) composed of kaolinite-like structures with clay- and sand-size particle deposits under TF (2B) and (2b). Under TF (2C) and RP (2c), occluded light fractions (OLF) are consisted of weakly bound light fractions with mineral particles. Light fractions (LF) at TF (2D) is composed large amount of plant residues compared to RP (2d).

cm layer) of TF and RP, which showed that bulk soil (Fig. 1A and 1a) and HF (Fig. 1B and 1b) fractions of both TF and RP were mainly composed of indistinct organic materials bound by microaggregates and silt + clay clusters. Meanwhile, OLF fractions had crystalline particles and unidentifiable partially decomposed organic materials within the coarse fractions (Fig. 1C and 1c). In addition, the LF at TF was composed of mixtures of leaves and fine roots, while RP mainly consisted of leaf litters (Fig. 1D and 1d). Overall, SEM examination revealed that the magnitude of mineral associated organic matter increased with increasing density-size SOM fraction.

3.2. Distribution and decomposition of fractions by aggregate- and density-size

Soil physicochemical properties in the two land-use types at 0–10 and 10–20 cm layers are presented in Table 1. Soil texture in the study site was clay loamy. The average clay and silt content in TF (38% and 30%) were significantly ($F = 43.2$; $p < 0.05$) higher than in the RP (31% and 28%) in the 0–10 cm soil layer. Soils in RP had higher bulk density than those in TF in both soil layers. Soil pH in TF was significantly ($F = 12.8$; $p < 0.05$) lower than that in RP (Table 1). Among

Table 1

Soil physico-chemical (at 0–10 and 10–20 cm soil depth) characteristics in tropical rainforest (TF) and rubber plantation (RP) sites.

Soil characteristics	TF		RP	
Annual mean air temperature (°C)	22			
Annual mean precipitation (mm)	1557			
Soil parent material	Cretaceous yellow sandstone, ~ 1 m soil depth			
	0–10 cm	10–20 cm	0–10 cm	10–20 cm
Soil texture				
Sand (%)	31.63 ± 0.83 ^a	31.33 ± 0.99 ^a	40.10 ± 1.14 ^b	39.22 ± 1.03 ^b
Silt (%)	30.14 ± 0.81 ^a	29.79 ± 0.45 ^a	28.65 ± 0.13 ^b	27.34 ± 0.28 ^b
Clay (%)	38.21 ± 0.96 ^a	37.87 ± 0.52 ^a	31.25 ± 0.68 ^b	33.46 ± 1.92 ^b
Textural class	Clay loam		Clay loam	
Soil taxonomy				
GSCC	[†] Latosol	–	[‡] Latosol	–
WRB	Acric Ferralsols	–	Acric Ferralsols	–
USDA	Oxisol	–	Oxisol	–
[§] Annual mean soil temperature (°C)	21.91 ± 1.30	–	22.86 ± 1.85	–
[§] Annual mean soil water content (% v/v)	30.93 ± 3.47	–	27.05 ± 4.05	–
Bulk density (g. cm ⁻³)	1.27 ± 0.08 ^a	1.34 ± 0.05 ^a	1.42 ± 0.11 ^b	1.45 ± 0.13 ^b
pH (1:2.5 H ₂ O)	4.7 ± 0.42 ^a	4.9 ± 0.54 ^a	5.11 ± 0.21 ^b	5.23 ± 0.55 ^b
Total C (g. kg ⁻¹)	28.06 ± 3.67 ^a	18.93 ± 2.82 ^a	20.55 ± 2.09 ^b	11.31 ± 3.70 ^b
Total N (g. kg ⁻¹)	3.14 ± 0.71 ^a	2.44 ± 0.33 ^b	2.39 ± 0.17 ^a	1.58 ± 0.12 ^b
C/N	8.94 ± 0.46 ^a	7.79 ± 1.07 ^b	8.61 ± 1.04 ^a	7.16 ± 0.99 ^b
Calcium oxide (CaO, %)	1.83	2.20	4.63	4.47
Aluminum oxide (Al ₂ O ₃ , %)	6.93	8.31	13.97	14.68
Ferric oxide (Fe ₂ O ₃ , %)	0.06	0.04	0.15	0.13

Different superscript alphabetic letters indicate the significance of differences ($p < 0.05$) in mean comparison at same depth between sites, values are mean ($n = 3$) ± standard error.

GSCC, Genetic Soil Classification of China; WRB, World Reference Base for soil resources; USDA, The United States Department of Agriculture

[†]Tang et al., 2010; [‡]Zhou et al., 2016b

[§] Surface soil (0–10 cm), mean values for 2016–2017.

the land-use types, total C and N varied significantly ($F = 30.2$; $p < 0.05$), and was higher in TF in the 0–10 cm soil layer (Table 1).

Changes in soil aggregate stability indicators such as MWD and GMD in 0–10 and 10–20 cm soil layers in TF and RP are shown in Fig. 2a, b. The MWD was greater in TF than RP and significantly ($F = 19.7$, $p < 0.05$) varied with soil depth within land-use type (Fig. 2a). The MWD varied from 1829 μ m in RP to 2809 μ m in TF in the 0–10 cm soil layer, and likewise, MWD varied from 1625 μ m (RP) to 2309 μ m (TF) in the 10–20 cm soil layers (Fig. 2a). The average MWD ($F = 54.21$, $p < 0.05$) and GMD ($F = 20.09$, $p < 0.05$) varied significantly between TF and RP. The GMD was significantly ($p < 0.05$) lower at 10–20 cm soil depth in both TF and RP (Fig. 2b).

Fig. 3a and 3b shows the variation in the mass proportion (%) of fractions with different aggregate- and density-size, respectively, at 0–10 and 10–20 cm soil depth. LUC had significant ($F = 13.5$, $p < 0.05$) effects on the distribution of individual aggregate- and density-size fractions. The average percentage recovery of total aggregate- and density-size fractions in relation to their initial mass of bulk soil varied from 70 to 98%, respectively across land-use type and soil layer (Table S1). Among different aggregate-size fractions, 60% were macroaggregates ($> 250 \mu$ m) and 40% were microaggregates ($< 250 \mu$ m) in bulk soils of both TF and RP (Fig. 3a). Similarly, on average, density fractions showed that bulk soil was composed of 85% HF and 5% and 10% of OLF and LF, respectively. After conversion of TF to RP (0–10 cm), among density SOM fractions, HF ($F = 19.7$) and LF ($F = 10.4$) significantly decreased by 7.67% and 67.1%, respectively ($p < 0.05$) (Fig. 3b).

3.3. C and N partitioning among bulk, aggregate-, and density-size fractions of SOM

The variations in C, N, and C:N ratios of bulk, aggregate-, and density-size fractions at 0–10 and 10–20 cm soil depths in response to LUC are illustrated in Fig. 4 and 5a–b. The mean C and N content associated with bulk, aggregate-, and density-size SOM fractions significantly decreased after conversion of TF to RP ($p < 0.05$) (Fig. 5a–b

and Table 2). The C and N content in different density SOM fractions followed the same trend (LF $>$ OLF $>$ HF) in both TF and RP plots (Fig. 4a–f and Table 2). There was no significant change in bulk soil C:N ratio of both soil layers ($p > 0.05$) (Fig. 4g and Table 3). However, C/N ratio of microaggregates ($< 250 \mu$ m) were significantly ($p < 0.001$) increased following conversion of TF to RP (Fig. 4h and Table 3). In contrast, the C/N ratio decreased significantly among density SOM fractions in response to LUC at both soil depths ($p < 0.05$) (Fig. 4i and Table 3). Among aggregate-size fractions, C/N ratios were higher in the 0–10 cm soil layer than at 10–20 cm, while the opposite trend was observed across density SOM fractions under both land-use types (Fig. 4h–i).

Table 4 summarizes the correlations (r) between bulk soil C, N, and MWD proportions of aggregate- and density-size fractions and, aggregate-size and density fraction C and N across land-use types and soil depths. The bulk soil C ($r = 0.55$, $p < 0.05$) and N ($r = 0.36$, $p < 0.05$) had a significant positive correlation with MWD (Table 4). Furthermore, C and N content in macroaggregates and LF fractions showed a significant ($p < 0.001$) positive relationship with bulk soil C and N. Meanwhile, C and N content associated with aggregate- and density-size SOM fractions showed a significant positive correlation with MWD (Table 4).

3.4. $\delta^{13}\text{C}$ and $\delta^{15}\text{N}$ of bulk, aggregate-, and density-size fractions

Table 5 presents the shifts in $\delta^{13}\text{C}$ and $\delta^{15}\text{N}$ values of bulk soil and individual aggregate- and density-size fractions in response to LUC at 0–10 and 10–20 cm soil depths. The transition of TF to RP was associated with an increase in $\delta^{13}\text{C}$ but decrease in $\delta^{15}\text{N}$ (Table 5 and Figure S2). The bulk soil $\delta^{13}\text{C}$ was significantly ($p < 0.05$) enriched by -3.21‰ and -2.18‰ in the 0–10 and 10–20 cm soil layers, respectively, after conversion of TF to RP (Table 5). Meanwhile, after LUC, bulk soil $\delta^{15}\text{N}$ was significantly depleted by 1.45‰ and 1.49‰ at depths of 0–10 and 10–20 cm, respectively ($p < 0.01$). In response to LUC, the highest increase in $\delta^{13}\text{C}$ was recorded for OLF and macroaggregate ($> 250 \mu$ m) fractions at 0–10 cm soil depth (Table 5).

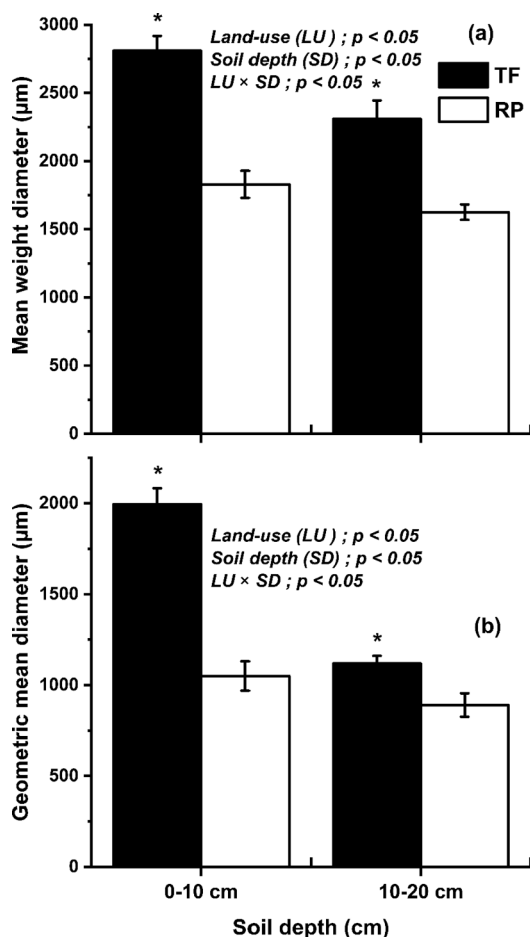


Fig. 2. The mean weight diameter (a) and geometric mean diameter (b) in tropical rainforest (TF) and rubber plantation (RP) at 0–10 and 10–20 cm soil depth. Vertical bars indicate the \pm standard error (SE) ($n = 3$). * indicates that values are significant at $p < 0.05$ between soil depth (SD).

Similarly, decrease in $\delta^{15}\text{N}$ was higher in OLF and macroaggregates fractions. The decrease in $\delta^{15}\text{N}$ was greater in the 10–20 cm soil layer, particularly in RP (Table 5).

The relationship between $\delta^{13}\text{C}$ and $\delta^{15}\text{N}$, and SOC and N of bulk soil, aggregate-, and density-size fractions across land-use types and soil depths are summarized in Table 6. The $\delta^{13}\text{C}$ and $\delta^{15}\text{N}$ were significantly ($p < 0.001$) correlated with aggregate- and density-size fractions associated C and N in all aggregate- (except for the 2000–250 μm) and density-size fractions across land-use types and soil depths (Table 6). The $\delta^{13}\text{C}$ and $\delta^{15}\text{N}$ values of HF and $> 2000 \mu\text{m}$ fractions established a significant negative correlation with C and N ($p < 0.001$).

4. Discussion

4.1. LUC effects on the stability of different SOM fractions

The mean total WSA and MWD decreased following the shift from TF to RP, primarily due to soil disruption by management related practices, while greater MWD in TF could be attributed to higher macroaggregates and C content (Handayani et al., 2010; Haghighi et al., 2010) (Fig. 2 and Fig. 3). This was confirmed by a significant positive relationship between MWD and C in aggregate- and density-size SOM fractions (Table 4). Substantiating our hypothesis, LUC stimulated the decomposition of macroaggregates as revealed by the decreasing proportion of macroaggregates (Fig. 3). A higher proportion of macroaggregates and HF in TF compared with RP could be due to the soil texture with higher silt and clay particles (68%, Table 1), which, in

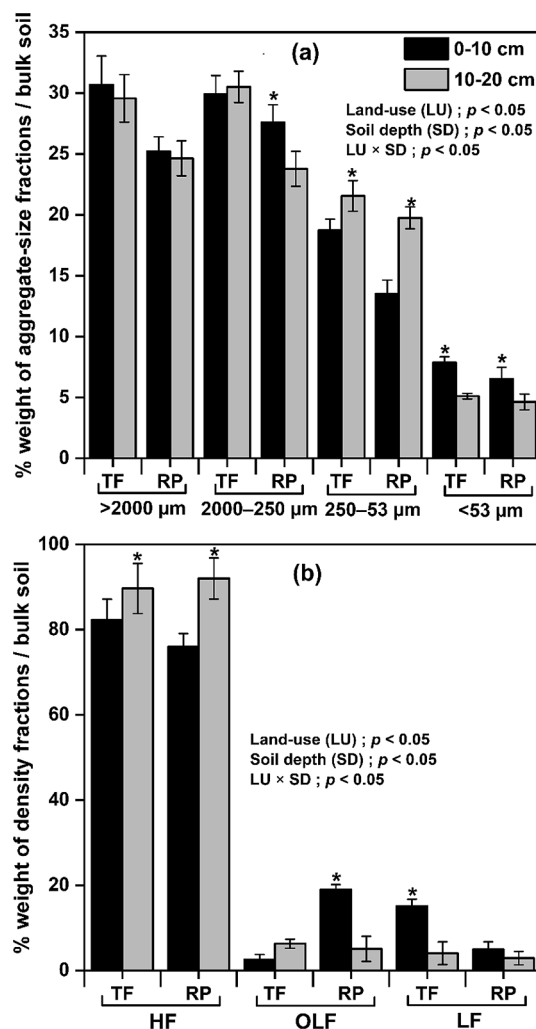


Fig. 3. Comparison of aggregate-size (a) and density (b) fractions in tropical rainforest (TF) and rubber plantation (RP). Vertical bars indicate the \pm SE ($n = 3$). HF, heavy fraction; OLF, occluded light fraction; LF, light fraction. * indicates that values are significant at $p < 0.05$ between soil depth (SD).

turn, adsorbs more SOM particles to form macroaggregates (Sollins et al., 1996).

The clay and silt particles ($< 53 \mu\text{m}$) act as binding agents of SOM to form macroaggregates (Powers et al., 2011), and clay and silt particles were significantly higher in TF than in RP ($F = 10.3$; $p < 0.05$) (Table 1). Fang and Sha (2005 and 2006) reported that the fine root biomass in RP (2551 kg hm^{-2}) was significantly lower than that in TF (6124 kg hm^{-2}), which also contributed to the decreased C content, MWD, and macroaggregates. Formation of macroaggregates was rapid when there were large quantities of easily available plant litters (Helfrich et al., 2006), while litter removal significantly decreased the proportion of macroaggregates (Blankinship et al., 2016). Soil capacity to maintain SOM aggregates in RP decreased subsequently as litter retention in RP dropped compared with that in TF (Zhang and Zhou, 2009).

Our results showed that the proportion of LF decreased following TF conversion to RP (Fig. 3), which indicated that LF was highly unstable and sensitive to LUC and management practices compared with the highly complex HF (Six et al., 2002). This is because LF is primarily composed of decomposed plant residues bound by transient binding agents: roots, fungal hyphae, and polysaccharides (Six et al., 2000; Cambardella and Elliott, 1994; Tisdall and Oades, 1982). Furthermore, SEM images revealed that LF was largely comprised of identifiable decomposing leaf and root litters in TF and mainly from leaf litters in

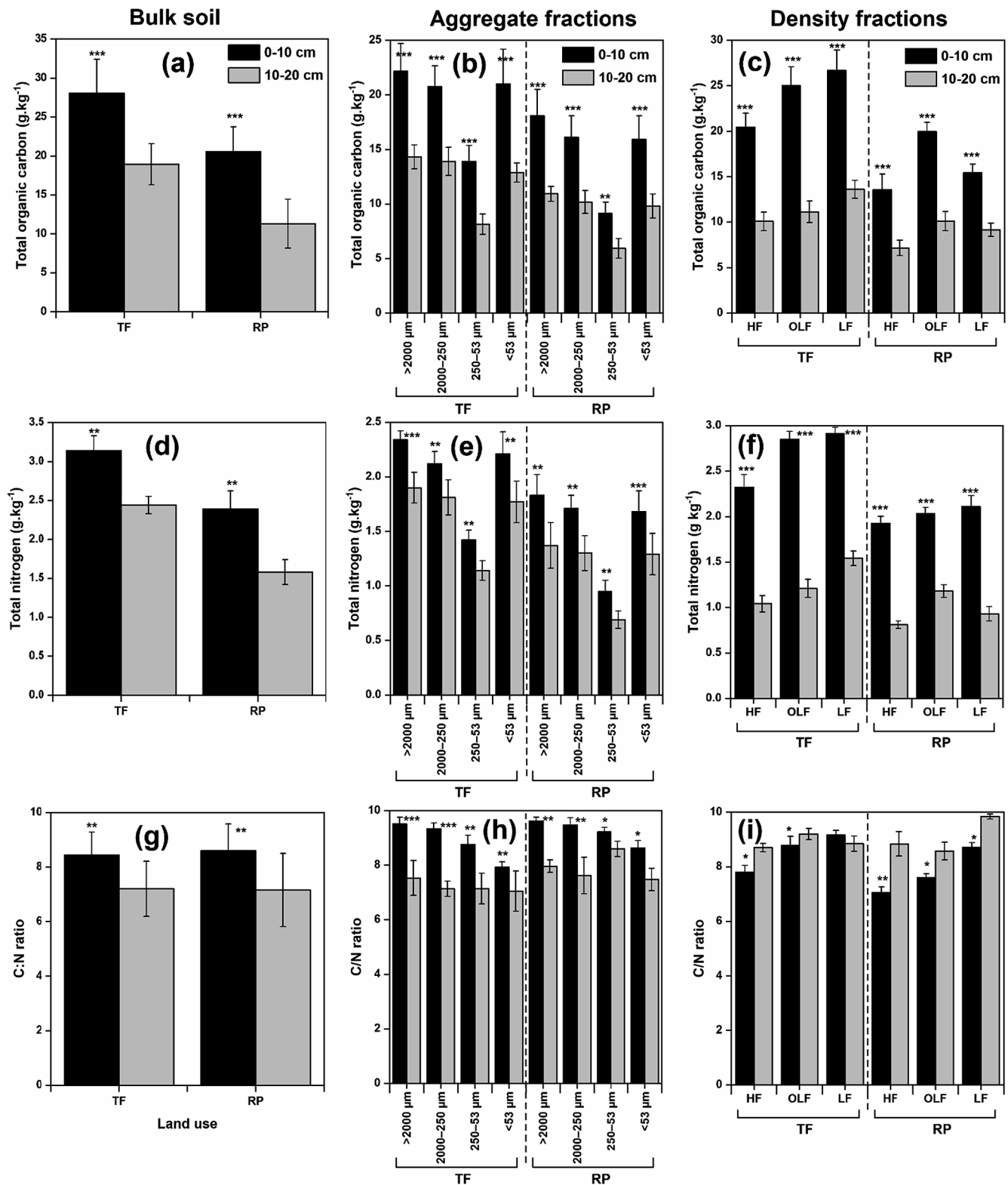


Fig. 4. Total organic carbon (a, b, c), total nitrogen (d, e, f) and C:N ratio (g, h, i) in bulk soil (left panel), aggregate-size (middle panel) and density (right panel) fractions across different soil depth (0–10 and 10–20 cm) under tropical rainforest (TF) and rubber plantation (RP). Vertical bars indicate the \pm SE (n = 3). ***, **, * indicates that values are significant at $p < 0.001$, $p < 0.01$, $p < 0.05$ respectively between soil depth (SD).

RP (Fig. 1D and 1d). The lower LF under RP plots could be primarily due to the magnitude and quality of litter input, whereas in TF, higher LF was due to a stable and higher amount of litter (Dou et al., 2016) and fine root (Fang and Sha, 2005) input.

New SOM aggregates formed from decomposing fine plant residues

(LF) are bound with resistant binding agents, such as oxides, at reactive surfaces (Gale et al., 2000; Tisdall and Oades, 1982). A review by Rowley et al. (2018) showed that Ca^{2+} , Al^{3+} , and Fe^{3+} can bridge SOM and associated minerals by adsorption on clay particles and occlusion within microaggregates, and denser HF at low pH (Rowley et al., 2018).

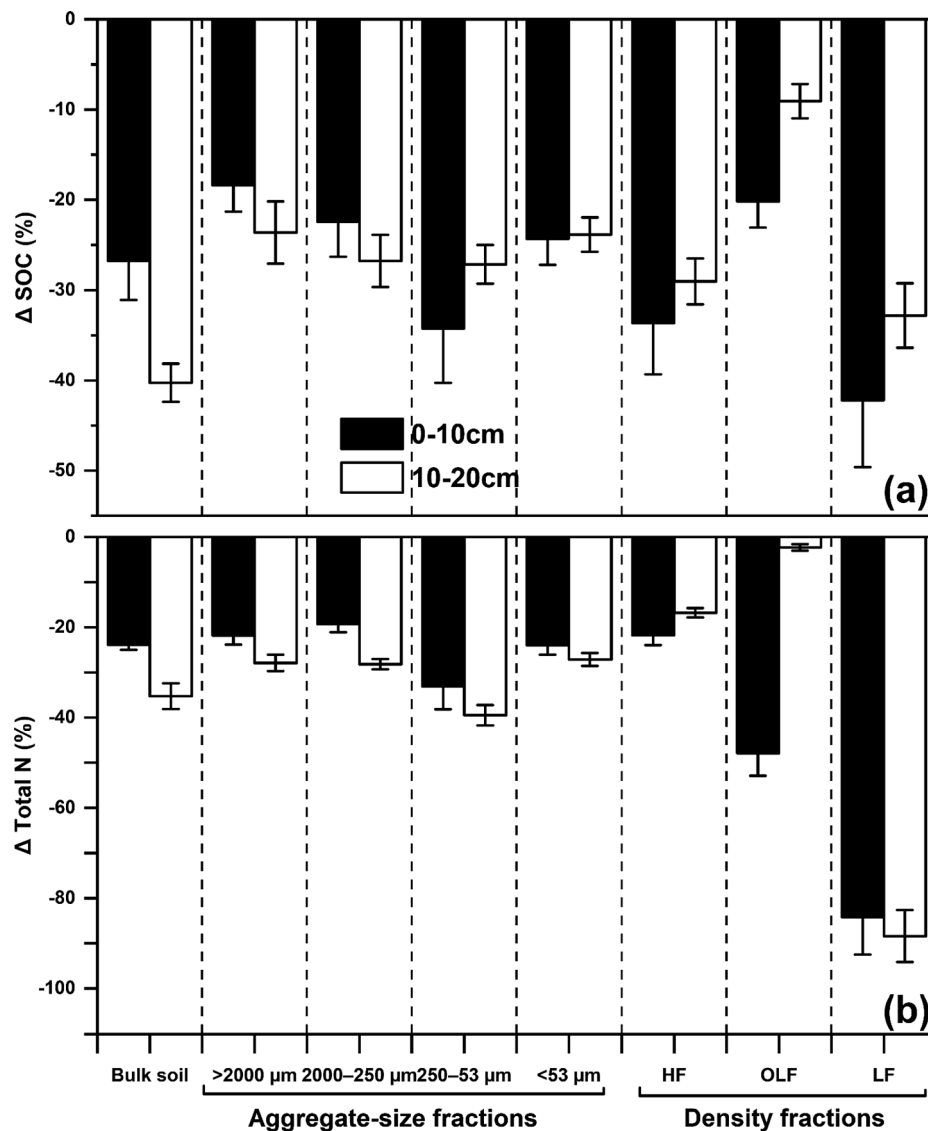


Fig. 5. Changes (Δ) in the SOC (a) and total N (b) at 0–10 cm and 10–20 cm soil depth in response to LUC from tropical rainforest (TF) to rubber plantation (RP). Vertical bars indicate the \pm standard error ($n = 3$).

Though, RP had higher CaO , Al_2O_3 and Fe_2O_3 content compared with TF at both 0–10 and 10–20 cm soil depth, clay content were significantly lower (Table 1). Consequently, higher clay content may explain the high SOM stability potential in TF compared with RP (Table 1). When macroaggregates and LF undergo microbial decomposition following LUC, preferential accumulation of labile SOM particles within microaggregates and HF occurs by occlusion, which can be mediated by Ca^{2+} , Al^{3+} , and Fe^{3+} . Microaggregates and HF have a higher surface area and lower C content that offer binding sites for negatively charged particles (Kramer et al., 2017). Thus, C and N within microaggregates and HF can be stabilized by forming humus–clay complexes through organo–mineral interactions mediated by Ca^{2+} , Al^{3+} , and Fe^{3+} (Rowley et al., 2018). The mechanisms underlying this SOM stabilization can be attributed to the capacity of Ca^{2+} , Al^{3+} , and Fe^{3+} for causing soil flocculation and bridging negatively charged molecules and clays. Hence, the effects of polyvalent cations (Al^{3+} and Fe^{3+}) on SOM stabilization needs to be specifically investigated further as Ca^{2+} highly likely are exchanged by Al^{3+} and Fe^{3+} in this acidic soil.

4.2. LUC effects on C and N within individual SOM fractions

C and N storage within bulk soil, as well as individual SOM fractions, significantly declined after LUC (Fig. 4a–i and Table 2 and Table S2). Corroboratively, the variation in SOM fraction chemistry between TF and RP soils suggests that LUC and management practices significantly affected C and N storage. Previous studies also confirmed that conversion of native forest to cultivated land rapidly diminished C and N content within SOM (Table S3). A few studies have reported LUC as a major driver of C and N loss under tropical rainforest to rubber plantation land-use change, e.g., in Indonesia (Kurniawan et al., 2018; Guillaume et al., 2015) and Ghana (Chiti et al., 2014). The high accumulation of litterfall and the undisturbed soil condition in TF resulted in higher C and N within the SOM fractions. Gmach et al. (2018) showed that litter input and undisturbed soil conditions promoted higher SOM aggregation and C and N stabilization. The importance of plant litter-derived C and N have been frequently reported in previous studies (e.g., Gale and Cambardella, 2000; Gale et al., 2000). According to Six et al. (2000) the formation of soil aggregates is strongly related to C, which was confirmed by the significant correlation between the proportion of SOM fractions and total C observed in the present study (Table 4).

Table 2

Percentage distribution and proportion of C and N among the different aggregate- and density-size fractions in tropical rainforest (TF) and rubber plantation (RP).

SOM fractions		TF		RP	
		0–10 cm	10–20 cm	0–10 cm	10–20 cm
Percentage	Aggregate-size fractions-C				
	> 2000 μm	28.46 \pm 2.48	29.07 \pm 3.22	30.52 \pm 3.90	29.67 \pm 2.46
	2000–250 μm	26.68 \pm 3.12	28.24 \pm 2.25	27.19 \pm 2.34	27.63 \pm 3.28
	250–53 μm	17.85 \pm 1.90	16.54 \pm 2.39	15.43 \pm 1.18	16.10 \pm 1.81
	< 53 μm	27.00 \pm 2.74	26.15 \pm 2.11	26.86 \pm 1.32	26.60 \pm 2.05
	Density-size fractions-C				
	HF	28.34 \pm 3.41	28.96 \pm 2.57	27.71 \pm 2.86	27.09 \pm 2.31
	OLF	34.67 \pm 2.98	31.95 \pm 2.84	31.51 \pm 3.44	34.62 \pm 2.40
	LF	36.99 \pm 5.02	39.09 \pm 3.08	40.78 \pm 3.67	38.29 \pm 3.09
	Aggregate-size fractions-N				
	> 2000 μm	26.41 \pm 2.60	28.70 \pm 2.26	29.66 \pm 3.15	29.46 \pm 3.10
	2000–250 μm	23.93 \pm 2.04	27.34 \pm 2.77	27.71 \pm 1.28	27.96 \pm 3.42
	250–53 μm	16.03 \pm 1.11	17.22 \pm 1.43	15.40 \pm 1.89	14.84 \pm 1.26
	< 53 μm	33.63 \pm 2.37	26.74 \pm 2.89	27.23 \pm 2.61	27.74 \pm 2.66
	Density-size fractions-N				
	HF	28.73 \pm 2.81	27.44 \pm 2.18	30.80 \pm 3.25	27.74 \pm 2.17
	OLF	35.26 \pm 2.93	31.93 \pm 4.01	32.52 \pm 3.11	31.85 \pm 2.64
	LF	36.01 \pm 4.01	40.63 \pm 4.52	36.68 \pm 3.26	40.41 \pm 3.97
Proportion	Aggregate-size fractions-C				
	> 2000 μm	78.97 \pm 1.12	75.59 \pm 2.16	87.98 \pm 3.05	96.64 \pm 3.10
	2000–250 μm	74.02 \pm 2.37	73.43 \pm 2.04	78.39 \pm 1.92	90.01 \pm 2.94
	250–53 μm	49.54 \pm 1.03	43.00 \pm 1.26	44.48 \pm 1.37	52.43 \pm 1.56
	< 53 μm	74.91 \pm 1.60	67.99 \pm 0.95	77.42 \pm 2.44	86.65 \pm 2.41
	Density-size fractions-C				
	HF	72.86 \pm 1.25	53.30 \pm 1.16	65.99 \pm 2.19	63.31 \pm 1.90
	OLF	89.11 \pm 2.87	58.80 \pm 1.20	75.04 \pm 2.31	80.90 \pm 2.35
	LF	95.07 \pm 2.63	71.95 \pm 1.41	97.12 \pm 2.85	89.48 \pm 3.05
	Aggregate-size fractions-N				
	> 2000 μm	74.52 \pm 1.25	77.87 \pm 1.25	76.57 \pm 1.33	86.71 \pm 2.35
	2000–250 μm	67.52 \pm 2.18	74.18 \pm 1.19	71.55 \pm 2.96	82.28 \pm 2.16
	250–53 μm	45.22 \pm 2.03	46.72 \pm 0.86	39.75 \pm 1.15	43.67 \pm 0.85
	< 53 μm	94.90 \pm 1.79	72.54 \pm 2.91	70.29 \pm 2.10	81.65 \pm 1.51
	Density-size fractions-N				
	HF	73.92 \pm 1.55	42.62 \pm 1.17	80.45 \pm 2.84	51.27 \pm 1.17
	OLF	90.73 \pm 2.09	49.59 \pm 1.15	84.94 \pm 2.39	58.86 \pm 1.64
	LF	92.68 \pm 2.20	63.11 \pm 1.70	88.28 \pm 2.71	74.68 \pm 1.42

n = 3, \pm SE; SOM, soil organic matter; C and N, carbon and nitrogen respectively

Among different aggregate-size fractions, a huge proportion of C and N was allocated to macroaggregates as well as microaggregates in both TF and RP in both soil layers. Likewise, the proportion of C and N was higher in LF fractions among density fractions. Thus, the decline in aggregate- and density-size fractions indicates that the large proportion of C and N also lost. This emphasizes the significance of SOM aggregates for maintaining soil structure and fertility. The loss of C and N occurred in both the surface and subsurface soil layers (Fig. 5 and Table S2). This means that stability and SOM aggregation of subsurface soil layers are also sensitive to LUC (Fig. 3). In the similar LUC condition, Guillaume et al. (2015) posited that variability in C and N losses vastly driven by the soil texture with high clay content. However, in the present study, we explain that the higher C and N losses from bulk soil, macro and microaggregates in RP (Fig. 5a-b and Table S2) could be primarily due to the soil disruption and long-term N fertilizer application in the two decades since LUC, because N addition promotes the turnover of SOM (Liu et al., 2018).

In spite of mechanical disturbance and soil erosion, C and N content within HF and < 53 μm aggregate fractions was higher (Fig. 4a-i). This could be due to the stabilization by physical and (bio)chemical protection (von Lützow and Kögel-Knabner, 2009). Furthermore, Fang et al. (2015) explained that spatial accessibility by microbes is lower due to the higher physical protection of C and N within the stable SOM fractions such as HF and < 53 μm sized fractions. With increasing decomposition rate, C and N within labile SOM pools could be adsorbed within the stabilized SOM fractions (Cheng et al., 2011). Another reason for higher C and N content within these stable SOM fractions was probably due to the adequate surface area for adsorbing and

accumulating more organic material (Fang et al., 2015).

Overall, our results suggest that stabilization of C and N could be predominantly driven by the occlusion into HF after LUC as shown by the significant increase in the proportion of OLF in RP (Fig. 3). The stabilization of SOM and its associated C and N by occlusion into HF is mediated by adsorption and complexation of SOM on the clay surfaces (Rabbi et al., 2010). This is due to the fact that occlusion of free SOM particles (from decomposing unstable LFs) into HF circumvent microbial and enzymatic degradation of SOM (von Lützow et al., 2008; Sollins et al., 1996). Thus, further research is warranted to understand the microbial diversity and extracellular enzyme activities in intra-aggregate SOM fractions.

C/N ratio had increased after conversion of TF to RP in both soil layers (Fig. 4g-i). As LUC alters the litter quality and quantity by changing species composition, the shifts in C/N ratios are expected in the present study, dependent upon the litter chemistry and quantity of litter input (Zhang and Zhou, 2009). Higher C/N ratio in LF and macroaggregates in the present study indicates the recently incorporated and incompletely decomposed litters (Kramer et al., 2017). Generally, in the present study, C/N ratio decreases with increasing density of SOM fractions, which in-turn implies the degree of decomposition and humification of SOM within HF. In previous research, Sollins et al. (1996) showed that when unstable labile SOM fractions decays, C is rapidly consumed by microbes compared with N and thereby decreases C/N ratios of LF and macroaggregate fractions. Thus, in our study, the C/N ratio found to indicate the SOM fractions capacity as both source and sink of C and N after LUC.

Table 3

The results of two-way ANOVA for the effects of land-use change (LUC) and soil depth (SD) on SOC contents, TN and C/N ratios, $\delta^{13}\text{C}$ and $\delta^{15}\text{N}$ in aggregate- and density-size fractions.

	Variables	SOM fractions	Source of variation LUC (df = 1)		SD (df = 1)		LUC*SD (df = 1)	
			F	p	F	p	F	p
AF	SOC	Bulk soil	17.221	0.003**	112.890	0.000***	17.911	0.003**
		> 2000 μm	10.327	0.040*	93.513	0.000***	40.226	0.000***
		2000–250 μm	56.903	0.000***	44.281	0.000***	13.408	0.001**
		250–53 μm	34.411	0.012*	12.088	0.001**	9.325	0.011*
		< 53 μm	46.192	0.000***	53.117	0.000***	12.152	0.004**
	TN	Bulk soil	13.814	0.001**	30.021	0.001**	1.129	0.388 ^{ns}
		> 2000 μm	9.565	0.003**	90.140	0.000***	51.039	0.002**
		2000–250 μm	67.452	0.052*	13.770	0.012*	8.243	0.012*
		250–53 μm	19.088	0.026*	37.213	0.000***	5.794	0.010*
		< 53 μm	8.162	0.000***	15.030	0.035*	21.366	0.005**
	C/N	Bulk soil	0.422	0.135 ^{ns}	0.957	0.894 ^{ns}	0.782	0.443 ^{ns}
		> 2000 μm	2.180	0.174 ^{ns}	3.214	0.652 ^{ns}	1.098	0.928 ^{ns}
		2000–250 μm	1.423	0.097 ^{ns}	1.902	0.344 ^{ns}	0.564	0.411 ^{ns}
		250–53 μm	51.041	0.000***	2.377	0.780 ^{ns}	0.475	0.970 ^{ns}
		< 53 μm	30.111	0.000***	0.928	0.531 ^{ns}	1.992	0.641 ^{ns}
	$\delta^{13}\text{C}$	Bulk soil	19.840	0.029*	1.083	0.295 ^{ns}	0.470	0.945 ^{ns}
		> 2000 μm	2.536	0.750 ^{ns}	0.541	0.127 ^{ns}	0.312	0.879 ^{ns}
		2000–250 μm	9.239	0.002**	7.180	0.001**	6.544	0.01*
		250–53 μm	15.091	0.000***	6.121	0.001**	9.029	0.02*
		< 53 μm	81.643	0.000***	40.236	0.000***	14.871	0.004**
	$\delta^{15}\text{N}$	Bulk soil	21.048	0.003**	8.155	0.001**	1.073	0.253 ^{ns}
		> 2000 μm	3.152	0.081 ^{ns}	1.849	0.472 ^{ns}	0.845	0.560 ^{ns}
		2000–250 μm	11.493	0.001**	7.826	0.001**	1.013	0.419 ^{ns}
		250–53 μm	9.579	0.033*	6.525	0.021*	0.535	0.876 ^{ns}
		< 53 μm	21.332	0.000***	19.427	0.000***	7.449	0.004*
DF	SOC	HF	83.029	0.000***	215.673	0.000***	39.390	0.000***
		OLF	91.547	0.000***	150.901	0.000***	47.115	0.000***
		LF	55.391	0.000***	52.640	0.000***	20.286	0.000***
	TN	HF	8.128	0.012*	9.566	0.007**	7.963	0.005**
		OLF	23.096	0.000***	19.238	0.000***	19.922	0.000***
		LF	12.550	0.006**	25.804	0.005**	6.375	0.018*
	C/N	HF	9.679	0.005**	5.980	0.006*	3.087	0.295 ^{ns}
		OLF	6.523	0.031*	1.097	0.717 ^{ns}	3.493	0.981 ^{ns}
		LF	10.980	0.019*	7.332	0.013**	1.142	0.460 ^{ns}
	$\delta^{13}\text{C}$	HF	1.673	0.944 ^{ns}	6.170	0.003**	0.921	0.087 ^{ns}
		OLF	20.047	0.003**	13.012	0.050*	2.183	0.094 ^{ns}
		LF	9.341	0.021*	30.156	0.000***	0.340	0.614 ^{ns}
	$\delta^{15}\text{N}$	HF	6.922	0.039*	3.009	0.785 ^{ns}	1.081	0.492 ^{ns}
		OLF	11.504	0.007**	1.091	0.333 ^{ns}	0.995	0.028 ^{ns}
		LF	17.619	0.004**	0.984	0.092 ^{ns}	2.039	0.950 ^{ns}

SOC, soil organic carbon; TN, total nitrogen; AF, aggregate-size fractions; DF, density-size fractions; HF, heavy fraction; OLF, occluded light fraction; LF, light fraction; F, indicates the ratio of the variance; p, indicates probability value or significance; *, **, *** indicates F values significant at $p < 0.05$, $p < 0.001$, $p < 0.001$ respectively; ^{ns} indicates not significant.

4.3. $\delta^{13}\text{C}$ and $\delta^{15}\text{N}$ evidence for LUC effects on SOM fractions

The $\delta^{13}\text{C}$ and $\delta^{15}\text{N}$ values of density- and aggregate-size fractions were significantly increased in the following order: HF > OLF > LF and < 53 μm > 250–53 μm > 2000–250 μm > 2000 μm , respectively (Table 3 and 5). This suggests that the recent litter (fresh SOM) was translocated within the macroaggregates and LF (Fig. 1). Our results agree with those of Angers and Giroux (1996) who reported that $\delta^{13}\text{C}$ decreased with increasing aggregate-size fractions in meadow soil. The differences in the $\delta^{13}\text{C}$ following LUC could also be due to shifts in the plant and soil isotopic composition (Table 3 and Table S3). LF $\delta^{13}\text{C}$ and > 250 μm fractions (Table 5) were comparable to those of bulk soil, presumably because they mostly comprised recent plant litters (Fig. 1). The $\delta^{13}\text{C}$ values were significantly correlated with bulk soil, aggregate- and density-size fractions associated C content (Table 6).

Meanwhile, $\delta^{13}\text{C}$ and $\delta^{15}\text{N}$ values showed that HF and < 53 μm aggregate fractions were the most enriched (Figure S2). Thus, decomposed and microbially processed SOM fractions were in HF and < 53 μm aggregates (Table 5). This suggests the wide variation in $\delta^{13}\text{C}$ values of different SOM fractions after LUC reflects differences in C turnover rates within particular SOM fractions (Table 5). In all aggregate- and density-size fractions, $\delta^{13}\text{C}$ enrichment was significantly

($p < 0.05$) greater at 10–20 cm than at 0–10 cm soil depth (Table 3 and 5). This could be due to enriching the $\delta^{13}\text{C}$ in subsurface soil, while microbial decomposition and preferential loss of light ^{12}C to CO_2 occurred in the surface SOM (Liu et al., 2018; Gunina and Kuzyakov, 2014).

Land-use and associated management practices have significantly affected C assimilation and transfer between SOM aggregate fractions. $\delta^{13}\text{C}$ values of individual SOM fractions registered a consistent positive shift (i.e., differences in $\delta^{13}\text{C}$ values of RP from that of the TF) from 1‰ to 2.5‰ at both soil depths after LUC (Figure S2a and S3). Isotope fractionation during SOM aggregates turnover (SOM stabilization and decomposition) resulted in enrichment of isotopic values of SOM fractions formed in subsequent phases. Liu et al. (2018) reported a direct relationship between SOM aggregate stabilization and C dynamics, suggesting that the higher abundance of $\delta^{13}\text{C}$ within microaggregates and HF could be due to the less-enriched $\delta^{13}\text{C}$ source. When fresh C (plant litters) enters the SOM system, it undergoes progressive microbial decomposition with preferential decomposition of lighter isotopes (^{12}C) thereby increasing the relative abundance of $\delta^{13}\text{C}$ in the remaining SOM (Liu et al., 2018; Gunina and Kuzyakov, 2014). Thus, by measuring the $\delta^{13}\text{C}$ abundance of individual SOM fractions, it would be possible to trace the C transfers between SOM fractions (Liu et al.,

Table 4

Pearson's correlation (*r*) between bulk soil C, N and MWD, and proportions of aggregate- and density-size fractions and C and N in aggregate-size and density fractions across land use types and soil depth.

Fractions	Bulk soil C 0–10 cm	10–20 cm	Bulk soil N 0–10 cm	10–20 cm	MWD 0–10 cm	10–20 cm
Proportion of AF						
> 2000 μm	0.843 ^{***}	0.416*	0.210 ^{ns}	0.181 ^{ns}	0.508*	0.394*
2000–250 μm	0.410*	0.302*	0.367*	0.295*	−0.207 ^{ns}	−0.173 ^{ns}
250–53 μm	0.386*	0.329*	0.491*	0.346*	0.294*	0.230 ^{ns}
< 53 μm	0.652*	0.270*	0.515 ^{**}	0.318*	0.569*	0.338*
Proportion of DF						
HF	0.672*	0.381*	0.598*	0.503*	0.447*	0.362*
OLF	0.315*	0.289*	0.171 ^{ns}	0.140 ^{ns}	−0.536*	0.411*
LF	0.428*	0.617*	0.556*	0.482*	0.580*	0.475*
Bulk soil						
Bulk soil C	–	–	0.870 ^{***}	0.537*	0.548*	0.451*
Bulk soil N	0.870 ^{***}	0.537*	–	–	0.363*	0.290*
AF-C						
> 2000 μm	0.592*	0.342*	0.478*	0.323*	0.812 ^{***}	0.619*
2000–250 μm	0.334*	0.316*	0.421*	0.295*	0.620*	0.503*
250–53 μm	−0.607*	−0.280*	−0.242 ^{ns}	−0.169 ^{ns}	0.706 ^{**}	0.526*
< 53 μm	0.290*	0.302*	0.417*	0.276*	0.833 ^{***}	0.741 ^{**}
DF-C						
HF	0.741 ^{**}	0.608*	−0.566*	−0.370*	0.867 ^{***}	0.809 ^{***}
OLF	−0.493*	−0.365*	−0.598*	−0.364*	0.402*	0.316*
LF	0.898 ^{***}	0.640*	0.815 ^{***}	0.789 ^{**}	0.698*	0.534*
AF-N						
> 2000 μm	0.487*	0.302*	0.505*	0.320*	0.527*	0.451*
2000–250 μm	0.540*	0.354*	−0.158 ^{ns}	−0.103 ^{ns}	0.330*	0.289*
250–53 μm	−0.319*	−0.281*	−0.112 ^{ns}	−0.096 ^{ns}	0.167 ^{ns}	0.121 ^{ns}
< 53 μm	0.662*	0.327*	0.276*	0.194 ^{ns}	−0.295*	−0.190 ^{ns}
DF-N						
HF	0.319*	0.314*	0.746 ^{**}	0.651 ^{**}	0.489*	0.315*
OLF	−0.307*	−0.371*	−0.194 ^{ns}	−0.127 ^{ns}	0.206 ^{ns}	0.148 ^{ns}
LF	0.495*	0.545*	0.377*	0.284*	−0.322*	−0.287*
AF-C:N						
> 2000 μm	0.378*	0.360*	0.846 ^{***}	0.710 ^{**}	0.537*	0.291*
2000–250 μm	−0.463*	−0.513*	0.455*	0.308*	−0.186 ^{ns}	−0.103 ^{ns}
250–53 μm	−0.540*	−0.219 ^{ns}	−0.608*	−0.453*	0.361*	0.217 ^{ns}
< 53 μm	−0.303*	−0.336*	−0.571*	−0.412*	−0.394*	−0.170 ^{ns}
DF-C:N						
HF	0.495*	0.348*	0.304*	0.231 ^{ns}	0.317*	0.167 ^{ns}
OLF	−0.255*	−0.246 ^{ns}	−0.425*	−0.210 ^{ns}	−0.309*	0.103 ^{ns}
LF	−0.341*	−0.150 ^{ns}	−0.459*	−0.204 ^{ns}	0.492*	0.256*

MWD, mean weight diameter; AF, aggregate-size fractions; DF, density fractions; C and N, soil organic carbon and total nitrogen respectively. HF, heavy fraction; OLF, occluded light fraction; LF, light fraction. *F*, indicates the ratio of the variance; *p*, indicates probability value or significance; *, **, *** indicates significant correlations at $p < 0.05$, $p < 0.001$, $p < 0.001$ respectively, ns, not significant

2018). In the present study, among aggregate-size fractions, C movement and stabilization followed C release by decomposition of macroaggregates to microaggregates (lower $\delta^{13}\text{C}$) and then to silt and clay particles ($\delta^{13}\text{C}$ enrichment) (Table 5). Similarly, among density fractions, the direction of SOM stabilization was from LF (lower $\delta^{13}\text{C}$) to OLF and to HF ($\delta^{13}\text{C}$ enrichment) (Table 5). The observed translocation of C between individual SOM fractions agrees with the scheme of C flows proposed by Gunina and Kuzyakov (2014) and Six et al. (2002).

The enrichment of $\delta^{13}\text{C}$ after LUC implies gradual mixing of old (TF) and new ^{13}C of SOC in RP (Guillaume et al., 2015). Corroborating our hypothesis: soil $\delta^{13}\text{C}$ and $\delta^{15}\text{N}$ abundance will shift after the LUC, the $\delta^{13}\text{C}$ enrichment after LUC reflects the older C mixing with fresh $\delta^{13}\text{C}$ depleted-C from current RP litters (Table 5 and Figure S3). Qiu et al. (2015) and Blagodatskaya et al. (2011) also reported similar $\delta^{13}\text{C}$ enrichment after LUC in tropical soils. This could be attributed to the preferential decomposition of easily available organic materials, whereas refractory SOM pools remain accrued with $\delta^{13}\text{C}$ (Gunina and Kuzyakov, 2014; Blagodatskaya et al., 2011).

Contradicting our first hypothesis, $\delta^{15}\text{N}$ depleted in both bulk soil and in all SOM fractions after LUC (Table 5 and Figure S3). The depletion of $\delta^{15}\text{N}$ may be associated with the application of large quantities of N fertilizers in RP (Qiu et al., 2015). Generally, N fertilizers are more depleted in $\delta^{15}\text{N}$ (< 0‰), and thereby, N deposition in RP might

have decreased the abundance of $\delta^{15}\text{N}$ (Bateman and Kelly, 2007). However, the most humified SOM fractions such as HF and micro-aggregate (< 53 μm) fractions had higher $\delta^{15}\text{N}$ (Table 5). Percolation of excess N fertilizer into subsurface soil layer elucidates the depletion of $\delta^{15}\text{N}$ in the 10–20 cm soil layers (Wright and Inglett, 2009; Qiu et al., 2015). Besides, inlying soil aggregate formation mechanisms such as adsorption of $\delta^{15}\text{N}$ depleted fertilizers on the surface of micro-aggregates and clay-silt aggregates could also result in $\delta^{15}\text{N}$ depletion.

5. Conclusions

The present study showed that both aggregate- and density-size fractionations significantly aided the separation of functional SOM fractions which could be employed as good early indicators of SOM stability after the LUC. Individual aggregate- and density-size fractions provided better insight than bulk soil into the physical and chemical shifts in response to LUC. The mean weight diameter, geometric mean diameter, and water stable aggregates proportion was greater in TF soil compared with those in RP. LUC significantly decreased C and N in bulk soil, aggregate-size, and density fractions and the overall stability of SOM. The losses in SOC and N from the bulk soil following LUC is mainly driven by the loss of proportion of macroaggregates (HF and LF). Overall, conversion of TF to monoculture RP enriched $\delta^{13}\text{C}$ but

Table 5The $\delta^{13}\text{C}$ and $\delta^{15}\text{N}$ values of bulk soil and individual aggregate- and density-size SOM fractions under TF and RP.

Isotopes	SOM fractions	TF		RP	
		0–10 cm	10–20 cm	0–10 cm	10–20 cm
$\delta^{13}\text{C}$ (‰)	A. Bulk soil	−24.91 ± 0.21	−24.85 ± 0.37	−23.70 ± 0.19	−23.67 ± 0.30
	B. Aggregate-size fractions				
	> 2000 μm	−25.31 ± 0.12	−23.75 ± 0.56	−23.62 ± 0.96	−23.57 ± 0.37
	2000–250 μm	−24.50 ± 0.05	−23.65 ± 0.37	−23.10 ± 0.48	−23.38 ± 0.21
	250–53 μm	−24.18 ± 0.38	−23.09 ± 0.51	−23.12 ± 0.55	−23.01 ± 0.56
	< 53 μm	−23.70 ± 0.19	−23.67 ± 0.25	−22.65 ± 0.52	−22.71 ± 0.34
	C. Density-size fractions				
	HF	−23.03 ± 0.81	−22.71 ± 0.33	−22.11 ± 0.46	−22.14 ± 0.91
	OLF	−25.64 ± 0.59	−22.62 ± 0.37	−23.13 ± 0.40	−22.18 ± 0.27
	LF	−26.10 ± 0.21	−24.80 ± 0.32	−24.58 ± 0.44	−24.64 ± 0.35
$\delta^{15}\text{N}$ (‰)	A. Bulk soil	3.91 ± 0.33	4.22 ± 0.10	2.46 ± 0.12	2.73 ± 0.13
	B. Aggregate-size fractions				
	> 2000 μm	3.52 ± 0.14	4.29 ± 0.21	2.43 ± 0.19	2.10 ± 0.57
	2000–250 μm	3.56 ± 0.19	4.17 ± 0.15	2.52 ± 0.34	2.19 ± 0.41
	250–53 μm	4.01 ± 0.28	5.50 ± 0.09	3.15 ± 0.15	2.35 ± 0.36
	< 53 μm	5.93 ± 0.15	5.81 ± 0.14	5.02 ± 0.27	2.56 ± 0.38
	C. Density-size fractions				
	HF	6.98 ± 0.21	6.79 ± 0.23	6.55 ± 0.39	3.01 ± 0.10
	OLF	5.22 ± 0.17	5.31 ± 0.21	3.58 ± 0.24	3.23 ± 0.37
	LF	3.85 ± 0.30	4.17 ± 0.26	2.84 ± 0.23	2.19 ± 0.15

TF, tropical rainforest; RP, rubber plantation; SOM, soil organic matter.

HF, heavy fraction; OLF, occluded light fraction; LF, light fraction.

Table 6The Pearson's correlation between $\delta^{13}\text{C}$ and $\delta^{15}\text{N}$, and SOC and total N of aggregate- and density-size fractions across land use types and soil depth.

Isotopes	SOM fractions	Aggregate-size and density fraction's SOC		TN		C/N	
		0–10 cm	10–20 cm	0–10 cm	10–20 cm	0–10 cm	10–20 cm
$\delta^{13}\text{C}$ (‰)	Bulk soil	0.309*	0.113 ^{ns}	0.288*	0.208 ^{ns}	0.251*	0.090 ^{ns}
	> 2000 μm	0.381*	0.279*	0.253*	0.128 ^{ns}	0.344*	0.212 ^{ns}
	2000–250 μm	−0.122 ^{ns}	−0.084 ^{ns}	0.147 ^{ns}	0.105 ^{ns}	0.308*	0.149 ^{ns}
	250–53 μm	0.267*	0.134 ^{ns}	0.365*	0.288*	0.316*	0.294*
	< 53 μm	0.434*	0.361*	0.390*	0.306*	0.250*	0.233 ^{ns}
	HF	0.335*	0.256*	−0.301*	−0.115 ^{ns}	0.279*	0.137 ^{ns}
	OLF	0.360*	0.293*	0.589*	0.363*	0.286*	0.180 ^{ns}
	LF	0.817***	0.380*	0.711**	0.415*	0.263*	0.141 ^{ns}
	Bulk soil	0.319*	0.157 ^{ns}	0.336*	0.289*	0.532*	0.217 ^{ns}
	> 2000 μm	0.496*	0.280*	0.310*	−0.170 ^{ns}	−0.329*	−0.201 ^{ns}
$\delta^{15}\text{N}$ (‰)	2000–250 μm	0.110 ^{ns}	0.073 ^{ns}	−0.142 ^{ns}	−0.083 ^{ns}	0.102 ^{ns}	−0.098 ^{ns}
	250–53 μm	0.574*	0.298*	0.446*	−0.227 ^{ns}	0.340*	0.236 ^{ns}
	< 53 μm	0.701**	0.355*	0.399*	−0.361*	0.616*	0.354*
	HF	0.552*	0.309*	0.647*	−0.323*	0.671*	0.554*
	OLF	0.373*	0.216 ^{ns}	0.590*	−0.379*	0.254*	0.189 ^{ns}
	LF	0.628*	0.240 ^{ns}	0.362*	−0.295*	−0.339*	−0.213 ^{ns}

SOM, soil organic matter; SOC and TN, soil organic carbon and total nitrogen respectively.

HF, heavy fraction; OLF, occluded light fraction; LF, light fraction.

*, **, *** indicates significant correlations at $p < 0.05$, $p < 0.001$, $p < 0.001$ respectively and ^{ns}, not significant.

depleted $\delta^{15}\text{N}$. A simple way to restore SOM quality and quantity could be planting intercrops within monoculture RP. To understand the C and N transfer among different SOM fractions upon LUC, future research should focus on molecular biochemical, physical, and chemical characterization of individual SOM fractions.

Declaration of Competing Interest

The authors declared that there is no conflict of interest.

Acknowledgments

This work was funded by the National Natural Science Foundation of China (31750110470, U1602234), the Chinese Academy of Sciences President's International Fellowship Initiative (CAS-PIFI) Grant No.

(2015PE007), China Postdoctoral Science Foundation (2016 M600754) and the Natural Science Foundation of Yunnan Province, China (2015FB188, 2016FB073). Fund from CAS 135 project (2017XTBG-F01) is also greatly acknowledged. Further, the authors thank all the staffs and technicians at the Public Technology Service Centre and the Xishuangbanna Station for Tropical Rainforest Ecosystem Studies of Xishuangbanna Tropical Botanical Garden, CAS, who contributed to soil analyses. Authors are thankful to the Central Laboratory of XTBG, especially to Prof. Fu Yun and Mr. Cao Li for isotopes measurements and to Mr. Ting Tang for SEM analysis of SOM fractions. We also thank Mr. Yang Donghai and all graduate students in the global change research group for their assistance in field works, soil samplings, and processing. We thank the anonymous reviewers and editors for their careful reading of our manuscript and their insightful comments and suggestions that greatly improved the manuscript.

Appendix A. Supplementary material

Supplementary data to this article can be found online at <https://doi.org/10.1016/j.catena.2020.104753>.

References

- Allen, S.E., 1989. *Chemical Analysis of Ecological Materials*, 2nd ed. Blackwell Scientific Publications, Oxford and London.
- Angers, D.A., Giroux, M., 1996. Recently deposited organic matter in soil water-stable aggregates. *Soil Sci. Soc. Am. J.* 60, 1547–1551. <https://doi.org/10.2136/sssaj1996.03615995006000050037x>.
- Bateman, A.S., Kelly, S.D., 2007. Fertilizer nitrogen isotope signatures. *Isot. Environ. Health Stud.* 43 (3), 237–247. <https://doi.org/10.1080/10256010701550732>.
- Blagodatskaya, E., Yuyukina, T., Blagodatsky, S., Kuzyakov, Y., 2011. Turnover of soil organic matter and microbial biomass under C3–C4 vegetation change: consideration of 13C fractionation and preferential substrate utilization. *Soil Biol. Biochem.* 43, 159–166. <https://doi.org/10.1016/j.soilbio.2010.09.028>.
- Blankinship, J.C., Fonte, S.J., Six, J., Schimel, J.P., 2016. Plant versus microbial controls on soil aggregate stability in a seasonally dry ecosystem. *Geoderma* 272, 39–50. <https://doi.org/10.1016/j.geoderma.2016.03.008>.
- Cambardella, C.A., Elliott, E.T., 1992. Particulate soil organic-matter changes across a grassland cultivation sequence. *Soil Sci. Soc. Am. J.* 56, 777–783. <https://doi.org/10.2136/sssaj1992.03615995005600030017x>.
- Cambardella, C.A., Elliott, E.T., 1994. Carbon and nitrogen dynamics of soil organic matter fractions from cultivated grassland soils. *Soil Science Soc. Am. J.* 58, 123–130. <https://doi.org/10.2136/sssaj1994.03615995005800010017x>.
- Cao, M., Zhang, J., Feng, Z., Deng, J., Deng, X., 1996. Tree species composition of a seasonal rain forest in Xishuangbanna. *Southwest China, Tropical Ecology* 37, 183–192.
- Cheng, X., Luo, Y., Xu, X., Sherry, R., Zhang, Q., 2011. Soil organic matter dynamics in a North America tallgrass prairie after 9 yr of experimental warming. *Biogeosciences* 8, 1487–1498. <https://doi.org/10.5194/bg-8-1487-2011>.
- Chiti, T., Grieco, E., Perugini, L., Rey, A., Valentini, R., 2014. Effect of the replacement of tropical forests with tree plantations on soil organic carbon levels in the Jomoro district, Ghana. *Plant Soil* 375, 47–59. <https://doi.org/10.1007/s11104-013-1928-1>.
- Christensen, B.T., 2001. Physical fractionation of soil and structural and functional complexity in organic matter turnover. *Eur. J. Soil Sci.* 52, 345–353. <https://doi.org/10.1046/j.1365-2389.2001.00417.x>.
- Cotrufo, F.M., Wallenstein, M.D., Boot, C.M., Denef, K., Paul, E., 2013. The Microbial Efficiency-Matrix Stabilization (MEMS) framework integrates plant litter decomposition with soil organic matter stabilization: do labile plant inputs form stable soil organic matter? *Glob. Change Biol.* 19, 988–995. <https://doi.org/10.1111/gcb.12113>.
- Dou, X., He, P., Zhu, P., Zhou, W., 2016. Soil organic carbon dynamics under long-term fertilization in a black soil of China: Evidence from stable C isotopes. *Sci. Rep.* 21488. <https://doi.org/10.1038/srep21488>.
- Fang, X., Chen, F., Wan, S., Yang, Q., Shi, J., 2015. Topsoil and deep soil organic carbon concentration and stability vary with aggregate size and vegetation type in subtropical China. *PLoS One* 10 (9), e0139380. <https://doi.org/10.1371/journal.pone.0139380>.
- Fang, Q.L., Sha, L.Q., 2005. Study of fine roots biomass and turnover in the rubber plantation of Xishuangbanna. *J. Central South University Forestry* 25, 40–44 (in Chinese with English abstract).
- Fang, Q.L., Sha, L.Q., 2006. Soil respiration in a tropical seasonal rainforest and rubber plantation in Xishuangbanna, Yunnan, SW China. *Acta Phytocologica Sinica* 30, 97–103 (in Chinese with English abstract).
- Frazão, L.A., Paustian, K., Pellegrino Cerri, C.E., Cerri, C.C., 2013. Soil carbon stocks and changes after oil palm introduction in the Brazilian Amazon. *Glob. Change Biol. Bioenergy* 5, 384–390. <https://doi.org/10.1111/j.1757-1707.2012.01196.x>.
- Gale, J., Cambardella, C.A., 2000. Carbon dynamics of surface residue- and root-derived organic matter under simulated no-till. *Soil Science Society America Journal* 64, 190–195. <https://doi.org/10.2136/sssaj2000.641190x>.
- Gale, J., Cambardella, C.A., Bailey, T.B., 2000. Root-derived carbon and the formation and stabilization of aggregates. *Soil Sci. Soc. Am. J.* 64, 201–207. <https://doi.org/10.2136/sssaj2000.641201x>.
- Gmach, M.-R., Dias, B.O., Silva, C.A., Nóbrega, J.C.A., Lustosa-Filho, J.F., Neto, M.S., 2018. Soil organic matter dynamics and land-use change on Oxisols in the Cerrado. *Brazil. Geoderma Regional* 4, e00178. <https://doi.org/10.1016/j.geodrs.2018.e00178>.
- Griepentrog, M., Schmidt, M.W.I., 2013. Discrepancies in utilization of density fractionation along with ultrasonic dispersion to obtain distinct pools of soil organic matter. *J. Plant Nutr. Soil Sci.* 176, 500–504. <https://doi.org/10.1002/jpln.201200469>.
- Guillaume, T., Damris, M., Kuzyakov, Y., 2015. Losses of soil carbon by converting tropical forest to plantations: Erosion and decomposition estimated by $\delta^{13}\text{C}$. *Global Change Biology* 21, 3548–3560. <https://doi.org/10.1111/gcb.12907>.
- Gunina, A., Kuzyakov, Y., 2014. Pathways of litter C by formation of aggregates and SOM density fractions: Implications from ^{13}C natural abundance. *Soil Biol. Biochem.* 71, 95–104. <https://doi.org/10.1016/j.soilbio.2014.01.011>.
- Haghighi, F., Gorji, M., Shorafa, M., 2010. A study of the effects of land use changes on soil physical properties and organic matter. *Land Degrad. Dev.* 21, 496–502. <https://doi.org/10.1002/ldr.999>.
- Handayani, L.P., Coyne, S., Tokosh, R.S., 2010. Soil organic matter fractions and aggregate distribution in response to tall Fescue stands. *International Journal of Soil Sciences* 5, 1–10. <https://doi.org/10.3923/ijss.2010.1.10>.
- Helfrich, M., Ludwig, B., Buurman, P., Flessa, H., 2006. Effect of land use on the composition of soil organic matter in density and aggregate fractions as revealed by solid-state C-13 NMR spectroscopy. *Geoderma* 136, 331–341. <https://doi.org/10.1016/j.geoderma.2006.03.048>.
- Jandl, G., Acksel, A., Baum, C., Leinweber, P., 2015. Indicators for soil organic matter quality under perennial crops in Central Sweden. *Soil Tillage Res.* 148, 74–84. <https://doi.org/10.1016/j.still.2014.12.006>.
- Kramer, M.G., Lajtha, K., Aufdenkampe, A., 2017. Natural abundance ^{15}N and C/N soil depth trends controlled more by association with minerals than by microbial decay. *Biogeochemistry Letters* 136 (3), 293–306. <https://doi.org/10.1007/s10533-017-0378-x>.
- Kurniawan, S., Corre, M.D., Matson, A.L., Schulte-Bisping, H., Utami, S.R., van Straaten, O., Veldkamp, E., 2018. Conversion of tropical forests to smallholder rubber and oil palm plantations impacts nutrient leaching losses and nutrient retention efficiency in highly weathered soils. *Biogeosciences* 15, 5131–5154. <https://doi.org/10.5194/bg-15-5131-2018>.
- Li, Y., Deng, X., Cao, M., Lei, Y., Xia, Y., 2013. Soil restoration potential with corridor replanting engineering in the monoculture rubber plantations of Southwest China. *Ecol. Eng.* 51, 169–177. <https://doi.org/10.1016/j.ecoleng.2012.12.081>.
- Liu, Y., Hu, C., Hu, W., Wang, L., Li, Z., Pan, J., Chen, F., 2018. Stable isotope fractionation provides information on carbon dynamics in soil aggregates subjected to different long-term fertilization practices. *Soil Tillage Res.* 177, 54–60. <https://doi.org/10.1016/j.still.2017.11.016>.
- Maggiotto, S.R., Oliveira, D.D., Marur, C.J., Stivari, S.M.S., Leclerc, M., Wagner-Riddle, C., 2014. Potential carbon sequestration in rubber tree plantations in the north-western region of the Paraná State, Brazil. *Acta Scientiarum: Agronomy* 36, 239–245. <https://doi.org/10.4025/actasciagron.v36i2.17404>.
- Moni, C., Derrien, D., Hatton, P.-J., Zeller, B., Kleber, M., 2012. Density fractions versus size separates: does physical fractionation isolate functional soil compartments? *Biogeosciences* 9, 5181–5197. <https://doi.org/10.5194/bg-9-5181-2012>.
- Oades, J.M., 1995. An overview of processes affecting the cycling of organic carbon in soils. In: Zepp, R.G., Sonntag, C.H. (Eds.), *Role of Nonliving Organic Matter in the Earth's Carbon Cycle*. John Wiley and Sons Ltd., pp. 293–303.
- Poeplau, C., Don, A., Vesterdal, L., Leifeld, J., Van Wesemael, B.A.S., Schumacher, J., Gensior, A., 2011. Temporal dynamics of soil organic carbon after land-use change in the temperate zone – carbon response functions as a model approach. *Glob. Change Biol.* 17, 2415–2427. <https://doi.org/10.1111/j.1365-2486.2011.02408.x>.
- Powers, J.S., Corre, M.D., Twine, T.E., Veldkamp, E., 2011. Geographic bias of field observations of soil carbon stocks with tropical land-use changes precludes spatial extrapolation. *Proc. Natl. Acad. Sci.* 108 (15), 6318–6322. <https://doi.org/10.1073/pnas.1016774108>.
- Qiu, L., Wei, X., Ma, T., Wei, Y., Horton, R., Zhang, X., Cheng, J., 2015. Effects of land-use change on soil organic carbon and nitrogen in density fractions and soil $\delta^{13}\text{C}$ and $\delta^{15}\text{N}$ in semiarid grasslands. *Plant Soil* 390, 419–430. <https://doi.org/10.1007/s11104-015-2435-3>.
- Rabbi, S.M.F., Lockwood, P.V., Daniel, H., 2010. How do microaggregates stabilize soil organic matter? In: *Proceedings of 19th World Congress of Soil Science, Soil Solutions for a Changing World 1 – 6 August 2010, Brisbane, Australia*. Published on DVD.
- Rahman, M.T., Liu, S., Guo, Z.C., Zhang, Z.B., Peng, X.H., 2019. Impacts of residue quality and N input on aggregate turnover using the combined ^{13}C natural abundance and rare earth oxides as tracers. *Soil Tillage Res.* 189, 110–122. <https://doi.org/10.1016/j.still.2019.01.005>.
- Rowley, M., Grand, S., Verrecchia, E., 2018. Calcium-mediated stabilisation of soil organic carbon. *Biogeochemistry* 137, 27–49. <https://doi.org/10.1007/s10533-017-0410-1>.
- Sierra, J., Desfontaines, L., 2018. Predicting the in situ rate constant of soil C mineralization from laboratory-based measurements in tropical soils under contrasting tillage management systems. *Soil Tillage Res.* 180, 175–181. <https://doi.org/10.1016/j.still.2018.03.008>.
- Six, J., Elliott, E.T., Paustian, K., Doran, J.W., 1998. Aggregation and Soil Organic Matter Accumulation in Cultivated and Native Grassland Soils. *Soil Sci. Soc. Am. J.* 62, 1367–1377. <https://doi.org/10.2136/sssaj1998.03615995006200050032x>.
- Six, J., Conant, R.T., Paul, E.A., Paustian, K., 2002. Stabilization mechanisms of soil organic matter: Implications for C-saturation of soils. *Plant Soil* 241, 155–176. <https://doi.org/10.1023/A:1016125726789>.
- Six, J., Elliott, E.T., Paustian, K., 2000. Soil macroaggregate turnover and microaggregate formation: a mechanism for C sequestration under no-tillage agriculture. *Soil Biology and Biochemistry* 32, 2099–2103. [https://doi.org/10.1016/S0038-0717\(00\)00179-6](https://doi.org/10.1016/S0038-0717(00)00179-6).
- Sohi, S.P., Mahieu, N., Arah, J.R.M., Powlson, D.S., Madari, B., Gaunt, J.L., 2001. A procedure for isolating soil organic matter fractions suitable for modelling. *Soil Sci. Soc. Am. J.* 65, 1121–1128. <https://doi.org/10.2136/sssaj2001.6541121x>.
- Sollins, P., Homann, P., Caldwell, B.A., 1996. Stabilization and destabilization of soil organic matter: Mechanisms and controls. *Geoderma* 74 (1–2), 65–105. [https://doi.org/10.1016/S0016-7061\(96\)00036-5](https://doi.org/10.1016/S0016-7061(96)00036-5).
- Tang, J.W., Cao, M., Zhang, J.H., Li, M.H., 2010. Litterfall production, decomposition and nutrient use efficiency varies with tropical forest types in Xishuangbanna, SW China: a 10-year study. *Plant Soil* 335, 271–288. <https://doi.org/10.1007/s11104-010-0414-2>.
- Tisdall, J.M., Oades, J.M., 1982. Organic Matter and Water-Stable Aggregates in Soils. *Eur. J. Soil Sci.* 33, 141–163. <https://doi.org/10.1111/j.1365-2389.1982.tb01755.x>.
- Trumbore, S., Brando, P., Hartmann, H., 2015. Forest health and global change. *Science* 349, 814–818. <https://doi.org/10.1126/science.aac6759>.
- Veldkamp, E., Purbopuspito, J., Corre, M.D., Brumme, R., Muriyarto, D., 2008. Land use change effects on trace gas fluxes in the forest margins of Central Sulawesi. *Indonesia*.

- Journal of Geophysical Research G02003. <https://doi.org/10.1029/2007JG000522>.
- von Lützow, M., Kögel-Knabner, I., 2009. Temperature sensitivity of soil organic matter decomposition-what do we know? *Biol. Fertil. Soils* 46, 1–15. <https://doi.org/10.1007/s00374-009-0413-8>.
- von Lützow, M., Kögel-Knabner, I., Ludwig, B., Matzner, E., Flessa, H., Ekschmitt, K., Guggenberger, G., Marschner, B., Kalbitz, K., 2008. Stabilization mechanisms of organic matter in four temperate soils: development and application of a conceptual model. *J. Plant Nutr. Soil Sci.* 171, 111–124. <https://doi.org/10.1002/jpln.200700047>.
- Wright, A.L., Inglett, P.W., 2009. Soil Organic Carbon and Nitrogen and Distribution of Carbon-13 and Nitrogen-15 in Aggregates of Everglades Histosols. *Soil Sci. Soc. Am. J.* 73, 427–433. <https://doi.org/10.2136/sssaj2008.0078>.
- Zandi, L., Erfanzadeh, R., Jafari, H.J., 2017. Rangeland use change to agriculture has different effects on soil organic matter fractions depending on the type of cultivation. *Land Degrad. Dev.* 28, 175–180. <https://doi.org/10.1002/ldr.2589>.
- Zhai, D., Xu, J., Dai, Z., 2015. Forest transition in Xishuangbanna. *Yunnan. Plant Diversity* 3 (1), 99–104. <https://doi.org/10.7677/ynzwjy201514051>.
- Zhai, D., Xu, J., Dai, Z., Schmidt-Vogt, D., 2017. Lost in transition: Forest transition and natural forest loss in tropical China. *Plant Diversity* 39 (3), 149–153. <https://doi.org/10.1016/j.pld.2017.05.005>.
- Zhang, M., Zhou, X.M., 2009. Comparison of soil C and N in rubber plantation and seasonal rain forest. *Chin. J. Appl. Ecol.* 20 (5), 1013–1019 (in Chinese with English abstract).
- Zhou, W.J., Sha, L.Q., Schaefer, D.A., Zhang, Y.P., Song, Q.H., Tan, Z.H., Deng, Y., Deng, X.B., Guan, H.L., 2015. Direct effects of litter decomposition on soil dissolved organic carbon and nitrogen in a tropical rainforest. *Soil Biol. Biochem.* 81, 255–258. <https://doi.org/10.1016/j.soilbio.2014.11.019>.
- Zhou, W.J., Lu, H.Z., Zhang, Y.P., Sha, L.Q., Schaefer, D.A., Song, Q.H., Deng, Y., Deng, X.B., 2016a. Hydrologically transported dissolved organic carbon influences soil respiration in a tropical rainforest. *Biogeosciences* 13, 5487–5497. <https://doi.org/10.5194/bg-13-5487-2016>.
- Zhou, W.J., Ji, H.L., Zhu, J., Zhang, Y.P., Sha, L.Q., Liu, Y.T., Zhang, X., Zhao, W., Dong, Y.X., Bai, X.L., Lin, Y.X., Zhang, J.H., Zheng, X.H., 2016b. The effects of nitrogen fertilization on N₂O emissions from a rubber plantation. *Sci. Rep.* 6, 28230. <https://doi.org/10.1038/srep28230>.